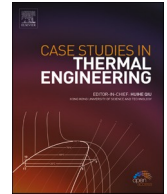




ELSEVIER

Contents lists available at ScienceDirect

Case Studies in Thermal Engineering

journal homepage: www.elsevier.com/locate/csite

Heat transport investigation of engine oil based rotating nanomaterial liquid flow in the existence of partial slip effect

Azad Hussain^a, Mubashar Arshad^a, Ali Hassan^a, Aysha Rehman^a, Hijaz Ahmad^b,
Jamel Baili^{c,d}, Tuan Nguyen Gia^{e,*}

^a Department of Mathematics, University of Gujrat, Gujrat, 50700, Pakistan

^b Section of Mathematics, International Telematic University Uninettuno, Corso Vittorio Emanuele II, 39, 00186, Roma, Italy

^c Department of Computer Engineering, College of Computer Science, King Khalid University, Abha, 61413, Saudi Arabia

^d Higher Institute of Applied Science and Technology of Sousse (ISSATS), Cité Taffala (Ibn Khaldoun) 4003 Sousse, University of Sousse, Tunisia

^e Department of Computing, University of Turku, 20500, Turku, Finland

ARTICLE INFO

Keywords:

Partial slip
Linear extending surface
Nanofluid
Rotational flow
Cu and Al₂O₃ nanoparticles

ABSTRACT

In this study, rotational nano liquid movement above a linearly stretching surface has been formulated. A two-phase model is used for this analysis. Base fluid engine oil and two distinct types of nanoparticles are used as nanoparticles, i.e. copper and aluminum oxide (Cu & Al₂O₃). This study is aimed to describe the changed possessions on velocity and temperature for rotational nanofluid flow above a linear enlarging surface in the existence of the slip effect. The leading structure of PDEs is converted into ODEs with a similarity transformation. Numerical findings are gained utilizing a sophisticated numerical approach. For both nanofluids, the results for rotational flow and heat transmission characteristics are emphasized with the help of graphs. At the linear extending surface, the influence of physical concentrations like heat flow rates and skin friction coefficients is investigated and visually clarified. Cu nanoparticles proved to be better heat carriers than Al₂O₃ nanoparticles.

1. Introduction

Flow problems caused by a linear expanding surface moving at a constant velocity arise often in a wide extent of industrial procedures. These sorts of flows are used in a variety of production processes, including the extraction of polymers from a dye, food preserving, chemical fluids, and so on. The primary phenomena of flowing across a linear expanding surface were initially observed by Crane [1]. Following that, this field of study was shown to be highly intriguing and being studied under different physical constraints. Wang [2] looked at viscid flow caused by a linearly stretching surface with suction and sliding effects. Dandapat and Gupta [3] examined the viscoelastic movement of fluid beyond the nonlinear extending sheet. Takhar and Nath [4] investigated the unstable rotating fluid flow over an extended surface with the magnetic field. Vajravelu and Hadjinicolaou [5] investigated heat transmission in a viscid fluid above an expanding sheet with heat creation and viscous degeneracy. Atefi et al. [6] analyzed at low and moderate Reynolds numbers, a numerical study of three-dimensional flow past a stationary sphere with slip condition. Hussain et al. [7–9] studied the 3D flow of different considerations above the linear stretching surface. Nadeem et al. [10] studied two-phase boundary

* Corresponding author.

E-mail addresses: azad.hussain@uog.edu.pk (A. Hussain), aysha.rehman@gim.edu.pk (A. Rehman), hijaz555@gmail.com (H. Ahmad), jabaili@kku.edu.sa (J. Baili), tunggi@utu.fi (T.N. Gia).

<https://doi.org/10.1016/j.csite.2021.101500>

Received 21 June 2021; Received in revised form 21 September 2021; Accepted 25 September 2021

Available online 5 October 2021

2214-157X/© 2021 The Authors. Published by Elsevier Ltd. This is an open access article under the CC BY license

(<http://creativecommons.org/licenses/by/4.0/>).

layer flow on a linearly stretching surface. Nima et al. [11] published fascinating research on the growing importance of nanofluids in a variety of technical and biomedical fields. Waini et al. [12] investigated heat transmission and unstable flow for hybrid nanofluid over an expanding surface.

First of all, Choi & Eastman [13] gave the concept of improving the thermal conductivity of fluids by using nanoparticles. The thermal conductivity of oxide nanoparticles was determined by Li and Eastman [14]. These types of fluids were found to be more efficient as compared to traditional heat transferring fluids like ethylene glycol engine oil, water, etc. Li et al. [15] generalized the heat transfer and temperature transmission of nanofluids with variable viscosity. Heat transport and hydrodynamic study of distributed fluids containing particles of metallic oxide were given by Pak and Choi [16].

The analytical conclusion of unsteady 3D magnetohydrodynamic (MHD) frontier layer movement and heat transfer was presented by Kumari & Nath [17]. Hussain et al. [18] described 3D flow over the rotating cone. Recently, Shafiq et al. [19] conducted research to characterize thermal and convective boundary slip in 3D flow. Zaimi et al. [20] investigated 3D viscoelastic flow over a stretching surface. Kumari & Nath [21] described the 3D transient rotating flow with magnetic effect over moving surface.

Takhar et al. [22] described flow and mass transmission on a stretched surface comprising chemically oxidants and a magnetic field. Mebarek-Oudina [23] studied the heat transmission of different base fluids with TiO_2 . Abbas et al. [24] studied heat and mass transfer for the unstable magnetohydrodynamic nanofluid flow through the porous medium past in the rotating apparatus. Hussain et al. [25] studied the hybrid nanofluid flow in the presence of the convective condition. Swain et al. [26] studied the hybrid nanoparticle's chemical reaction and slip boundary settings. Study of fluids has been investigated by several researchers [27–45] in response to new needs and applications. No one has characterized the combined properties of rotation and partial-slip of a nanofluid over an expanding surface to the best of our knowledge. Flows of this nature might be useful in a variety of applications in numeral up-to-date devices.

The foremost objective of this analysis is to investigate the heat transfer features and velocity of a spinning nanofluid over an extended surface in the presence of a partial slip effect using computational methods. To solve the problem, a physical model, namely the two-phase nanofluid model, was utilized. The powerful approach is utilized to get numerical outcomes and graphs. Velocity, temperature, and skin friction constants are calculated, confirmed visually, and deliberated concerning the dimensionless slip parameter K , volume fraction ϕ , and rotation parameter λ . Cu and Al_2O_3 - Nanoparticles were chosen for this comparative investigation because they had higher and lower densities, respectively, and no one has ever proven a slip impact with engine oil, to the best of our knowledge.

2. Statement of problem

Consider with a constant density engine oil-based rotational nanofluid laying above a flat stretchable surface in region $z \geq 0$ along the z - axis with fixed rotation rate Ω . Two identical and opposing forces are functional along the x -axis, causing the surface to stretch at a speed $U(x)$, which is precisely proportional to the distance from the origin at $x = 0$. Slip flow conditions are applied to the nanofluid. There is no external force acting on the nanofluid, therefore it is subject to slip flow conditions.

3. Equations and mathematical expressions

The problem's geometry is depicted in Fig. 1. The resulting energy and momentum equations [46] are obtained after ignoring the pressure gradient and viscous dissipation.

$$\frac{\partial u}{\partial x} + \frac{\partial v}{\partial y} + \frac{\partial w}{\partial z} = 0, \quad (1)$$

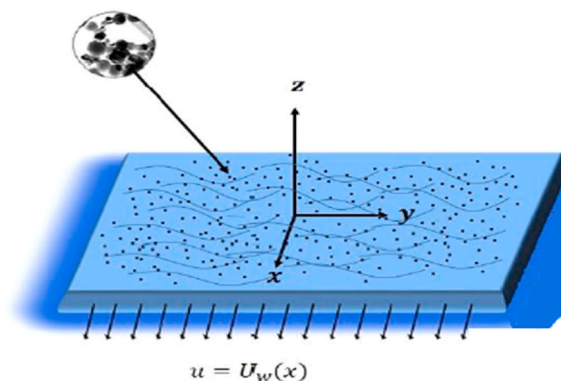


Fig. 1. Geometry of the problem.

$$u \frac{\partial u}{\partial x} + v \frac{\partial u}{\partial y} + w \frac{\partial u}{\partial z} = 2\Omega v + \frac{\mu_{nf}}{\rho_{nf}} \nabla^2 u, \tag{2}$$

$$u \frac{\partial v}{\partial x} + v \frac{\partial v}{\partial y} + w \frac{\partial v}{\partial z} = -2\Omega u + \frac{\mu_{nf}}{\rho_{nf}} \nabla^2 v, \tag{3}$$

$$u \frac{\partial w}{\partial x} + v \frac{\partial w}{\partial y} + w \frac{\partial w}{\partial z} = \frac{\mu_{nf}}{\rho_{nf}} \nabla^2 w, \tag{4}$$

$$u \frac{\partial T}{\partial x} + v \frac{\partial T}{\partial y} + w \frac{\partial T}{\partial z} = \alpha_{nf} \frac{\partial^2 T}{\partial z^2}. \tag{5}$$

Here $u, v,$ and w are x, y and z constituent of velocity Ω, μ_{nf} is fluid’s viscosity (dynamic), ρ_{nf} is nanofluid’s density, α_{nf} is temperature diffusiveness of the nanofluid, T is nanofluid’s temperature, $(\rho C_p)_{nf}$ is volumetric temperature capability of nanofluid, $(\rho C_p)_f$ is volumetric heat capability of base fluid, $(\rho C_p)_s$ is the volumetric heat capacity of solid nanoparticles. As seen below, all of these are connected to the [46] particle concentration φ of nanoparticles.

$$\left. \begin{aligned} \mu_{nf} &= \frac{\mu_f}{(1-\varphi)^{\frac{2.5}{\varphi}}}, \\ \rho_{nf} &= \rho_f(1-\varphi) + \varphi\rho_s, \\ (\rho C_p)_{nf} &= (\rho C_p)_f(1-\varphi) + \varphi(\rho C_p)_s, \\ \alpha_{nf} &= \frac{k_{nf}}{(\rho C_p)_{nf}}, \\ \nu_{nf} &= \frac{\mu_{nf}}{\rho_{nf}}, \\ \frac{k_f}{k_{nf}} &= \frac{k_s + 2k_f + 2\varphi(k_f - k_s)}{k_s + 2k_f - 2\varphi(k_f - k_s)}. \end{aligned} \right\} \tag{6}$$

Here, the base fluid’s thermal conductivity is k_f , temperature conductivity of solid nanoparticles is k_s, ρ_s is solid nanoparticles density and ρ_f is base fluid density.

The corresponding boundary conditions are given below.

$$\left. \begin{aligned} u(x, y, 0) - U &= kv \frac{\partial u}{\partial z}(x, y, 0), \\ v(x, y, 0) &= kv \frac{\partial v}{\partial z}(x, y, 0), \\ w(x, y, 0) &= kv \frac{\partial w}{\partial z}(x, y, 0). \end{aligned} \right\} \tag{7}$$

Where $U = ax$ is the surface extension velocity, $“a”$ is the surface enlarging rate, k is the slip distance, and ν is the kinematic viscosity of the base fluid.

3.1. Transformation methodology

Using the similarity transformation, which is as follows:

$$\left. \begin{aligned} u &= axf'(\eta), v = axh(\eta), w = -\sqrt{av} \\ f(\eta) &= z\sqrt{\frac{a}{\nu}}, \\ \theta(\eta) &= \frac{T - T_\infty}{T - T_w}. \end{aligned} \right\} \tag{8}$$

Here η is the non-dimensional constraint, temperatures at the wall and free streams are T_w and T_∞ respectively.

We can see that when we use this Eq. (8) in Eq. (1), it stays the same, i.e. mass is conserved. Eqs. (2)–(5) are converted into ODEs as follows by using values from Eqs. (6) and (8).

$$f''' + (1 - \varphi)^{5/2} \left(1 - \varphi + \frac{\rho_s}{\rho_{bf}} \varphi \right) (2h\lambda + ff'' - f'^2) = 0, \tag{9}$$

$$h'' + (1 - \varphi)^{5/2} \left(1 - \varphi + \frac{\rho_s}{\rho_{bf}} \varphi \right) (fh' - hf' - 2\lambda f') = 0, \tag{10}$$

$$\frac{k_{nf}}{k_f} \theta''(\eta) + Pr \left[1 - \varphi + \frac{(\rho C_p)_s}{(\rho C_p)_f} \varphi \right] f \theta'(\eta) = 0. \tag{11}$$

In these Eqs. (9)–(11), rotation constraint is λ and Prandtl number is Pr which is defined as

$$Pr = \frac{(\mu C_p)_f}{k_f}, \lambda = \frac{\Omega}{a}. \tag{12}$$

The fixed angular fluid’s velocity is determined by the preceding formulae. The complying boundary conditions are formed by using Eq. (8) into Eq. (7), we get

$$\left. \begin{aligned} f(0) = 0, f'(0) = 1 + Kf''(0), f'(\infty) = 0, \\ h(0) = K h'(0), h(\infty) = 0, \theta(0) = 1, \theta(\infty) = 0. \end{aligned} \right\} \tag{13}$$

The slip parameter is $K = K\sqrt{av}$.

3.2. Method of solution

The nonlinearity of the coupled system of ordinary differential equations (9)–(11) has been handled numerically. The technique transforms the arising differential equations into a set of first-order ordinary differential equations that are solved iteratively. The powerful software MATLAB is used to gain graphical results and numerical tables. Physical extents of our distinct comforts are skin frictions (Cf_x, Cf_y) along with the x – axis, y – axis respectively, and Nu Nusselt number, where

$$\left. \begin{aligned} Cf_x &= \frac{\tau_{xz}}{\rho(ax)^2}, \\ Cf_y &= \frac{\tau_{yz}}{\rho(ax)^2}, \\ Nu &= \frac{xq_w}{k_f(T - T_\infty)}. \end{aligned} \right\} \tag{14}$$

Where q_w is the heat flux, τ_{xz} and τ_{yz} denote the surface shear stresses respectively.

$$\left. \begin{aligned} \tau_{xz} &= \mu_{nf} \left(\frac{\partial u}{\partial z} + \frac{\partial w}{\partial x} \right)_{z=0}, \\ \tau_{yz} &= \mu_{nf} \left(\frac{\partial v}{\partial z} + \frac{\partial w}{\partial y} \right)_{z=0}, \\ q_w &= -k_{nf} \left(\frac{\partial T}{\partial z} \right)_{z=0}. \end{aligned} \right\} \tag{15}$$

By substituting equation (8) and equation (15) in equation (14), we get

$$\left. \begin{aligned} (Re_x)^{1/2} Cf_x &= \frac{1}{(1 - \varphi)^{5/2}} f''(0), \\ (Re_x)^{1/2} Cf_y &= \frac{1}{(1 - \varphi)^{5/2}} h'(0), \\ (Re_x)^{-1/2} Nu &= \frac{-k_{nf}}{k_f} \theta'(0). \end{aligned} \right\} \tag{16}$$

Where $Re_x = \frac{(ax)x}{\nu_f}$ is Reynolds number. Skin friction $\frac{1}{(1 - \varphi)^{5/2}} f''(0)$ and heat transmission $\frac{-k_{nf}}{k_f} \theta'(0)$ are premeditated for both types of nanofluid with distinct values of volume concentration φ , rotation constraint λ , and slip parameter. K .

4. Figures and tables

The effect of various physical parameters such as rotation constraint λ , volume concentration φ , and slip parameter K on velocity profiles and temperature for Al_2O_3 as well as Cu Engine oil nanofluid is discussed in this section. To assess their genuine impact on these physical extents, graphical results are achieved. For this reason, the following figures are plotted.

Fig. 2(a) and 2(b) are designed to conclude the impact on the velocity profile $f'(\eta)$ of slip constraint K and the rotation constraint λ for Cu and Al_2O_3 -Engine oil nanofluid respectively. To rise slip constraint K , results can be seen from Fig. (2a) in a substantial increase in the velocity profile $f'(\eta)$ for both Cu and Al_2O_3 -Engine oil nanofluid. It is because, when there is a slip, the speed of fluid close the surface does not match the enlarging of the surface. As a result, raising the slip parameter K , increases slip velocity. As a result, fluid velocity diminishes in this case, drawing of stretching surface only in a partial way can be because of slip factor presence. Also, the slip parameter rises, the boundary layer thickness decreases. Though interesting to know about the insertion of Cu nanoparticles shows a decline in the velocity profile $f'(\eta)$, and the way of behaving is contrary for Al_2O_3 nanoparticles (see Fig (2a)). This comes from the fact that Al_2O_3 nanoparticles are slighter in density as weigh up to the Cu nanoparticles. Therefore their addition in base fluid compromises a smaller amount of friction comparatively.

Correspondingly, it can be distinguished that from Fig (2b) an increment in the rotation constraint λ drops the velocity profile $f'(\eta)$ for both kinds of particles. It is because of the velocity slip existence feature which dominates the movement of fluid linked with rising rotation.

The effect of rotation λ and partial slip K on velocity component $h(\eta)$ is shown in Fig. 3(a) and 3(b) for both Cu and Al_2O_3 -Engine oil nanofluids. In Fig (3a) it is obvious that the velocity profile $h(\eta)$ decays as the slip constraint K rises to close the wall. Although it can be seen that for both nanofluids the velocity profile is decreasing but rising slip-on wall decreases thermal boundary in y-direction more rapidly for Cu -Engine oil as compared to Al_2O_3 -Engine oil. Also, it can be observed that the impact of particle volume concentration φ is reverse on $h(\eta)$ for Al_2O_3 and Cu -Engine oil fluid.

Fig (3b) presents velocity profile $h(\eta)$ for instant decays with a rise in rotation parameter λ , but after a gradual increase in rotation parameter, the velocity profile can be seen increasing. This specific manner is noted to be similar for both Al_2O_3 and Cu -Engine oil nanofluid. The physically thermal frontier layer at first has decreased but increases with the increase in rotation parameter λ .

By Fig. 4(a) and 4(b) it can be noted that the velocity profile $f(\eta)$ upsurges by rising slip constraint K and declines by rising rotation constraint λ . Moreover, with the inclusion of Cu nanoparticles, flow profile $f(\eta)$ decays while it increases for Al_2O_3 nanoparticles. This is due to the higher and lower density of copper and aluminum oxide particles respectively.

Fig. 5(a) and 5(b) demonstrate a difference in temperature profile $\theta(\eta)$ against slip K and volume fraction φ Cu and Al_2O_3 -Engine oil. It's worth noting that the temperature profile $\theta(\eta)$ is unaffected by the rotation constraint λ . We can note from Fig. 5(a) that temperature profile $\theta(\eta)$ significantly drops with a rise in slip parameter K and rises with an increase in volume fraction φ Fig (5b) due to good thermal conductivity of engine oil-based nanofluids.

The following tables are generated to inspect the dissimilarities of intriguing physical parameters on the skin friction constant and Nusselt number. Thermophysical characteristics of nanofluid and nanoparticles are shown in Table 1. By Table 2, it can be illustrated that for a specific value of rotation constraint λ , skin friction $\frac{1}{(1-\varphi)^{5/2}} f''(0)$ and temperature flux $\left(\frac{-kf}{k_f}\right) \theta'(0)$ rises with a rise of volume concentration φ , for both nanofluids. This is due to the inclusion of solid nanoparticles in the base fluid, it comes to be thicker and

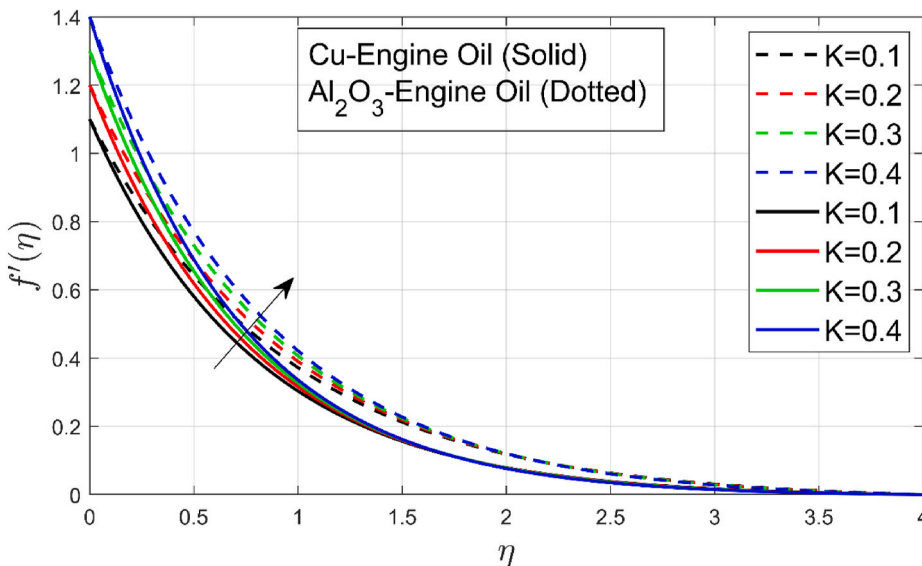


Fig. 2(a). The impact of slip K on velocity $f'(\eta)$

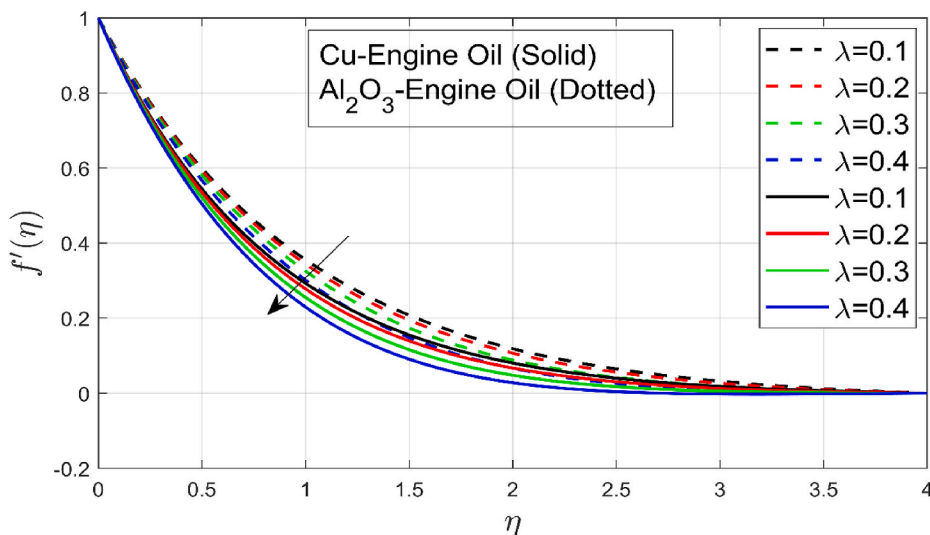


Fig. 2(b). The impact of rotation λ on velocity $f'(\eta)$

results in additional friction. While nanoparticles have greater thermal conductivity as compared to base fluid, the heat transmission rate increases compared to the pure base fluid. Notably, corresponding values of skin friction and temperature flux are dissimilar for Cu and Al_2O_3 – Engine oil which indicates the significance of the types of nanoparticles. Further, for fixed volume concentration ϕ , while rising slip K , decreases the skin resistance and heat flux for both nanofluids. This is due to an increase in slip clues to increase surface friction and ultimately rises heat flux at the wall. We noted that skin friction of Cu – Engine oils is always higher than Al_2O_3 – Engine oil due to the higher density of Cu related to Al_2O_3 nanoparticles. On the other side, Cu – Engine oil is verified to be more capable in rapid transmission of heat from the wall because of having high-temperature conductivity and higher specific heat capacity as associated with Al_2O_3 – Engine oil nanofluid. The impact of rotation λ and volume concentration ϕ on skin friction and heat transmission is presented in Table 3 for both nanofluids. We noticed that increasing the rotation λ results in a decrease in skin friction and an increase in heat transmission. This behavior is similar for both Cu and Al_2O_3 - Engine oil nanofluid. It is because a rise in rotation λ for fixed slip K results in lower resistance at the surface. Table 4 and 5 are tabulated to endorse the precision of current results. It is originated that our outcomes for skin friction and Nusselt number are in good agreement with the already published works. Fig. 6(a) and 6(b) show graphical representations for skin friction and Nusselt number.

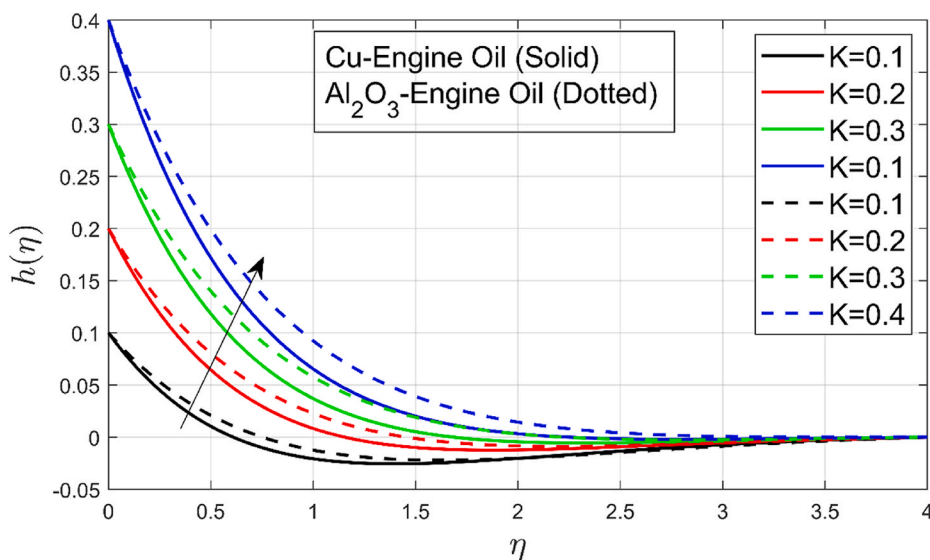


Fig. 3(a). The impact of slip K on velocity $h(\eta)$

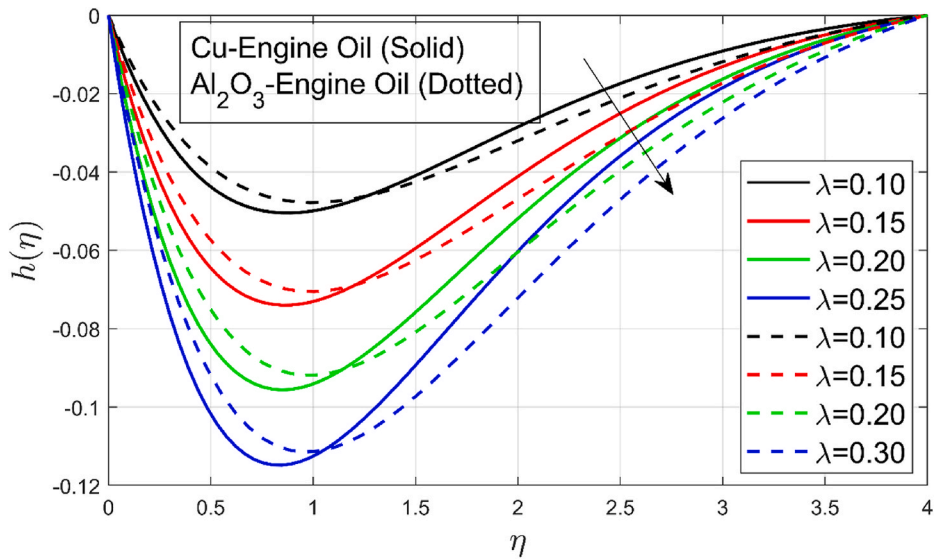


Fig. 3(b). The impact of rotation λ on velocity $h(\eta)$

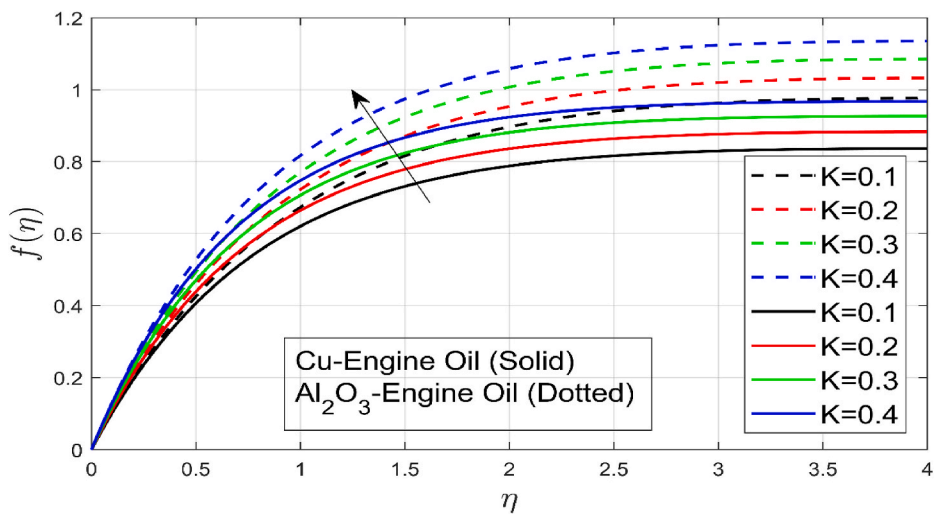


Fig. 4(a). The impact of slip K on velocity $f(\eta)$

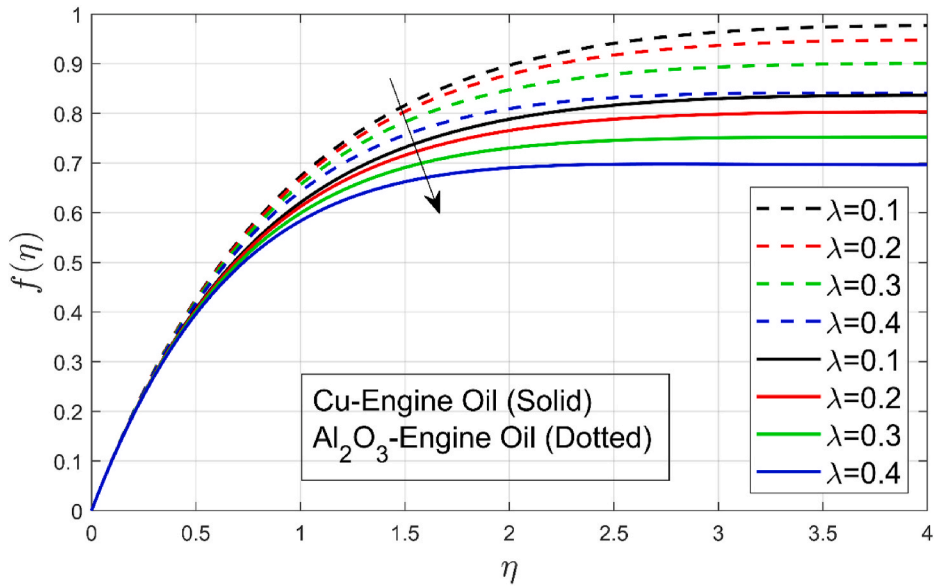


Fig. 4(b). The impact of rotation λ on velocity $f(\eta)$.

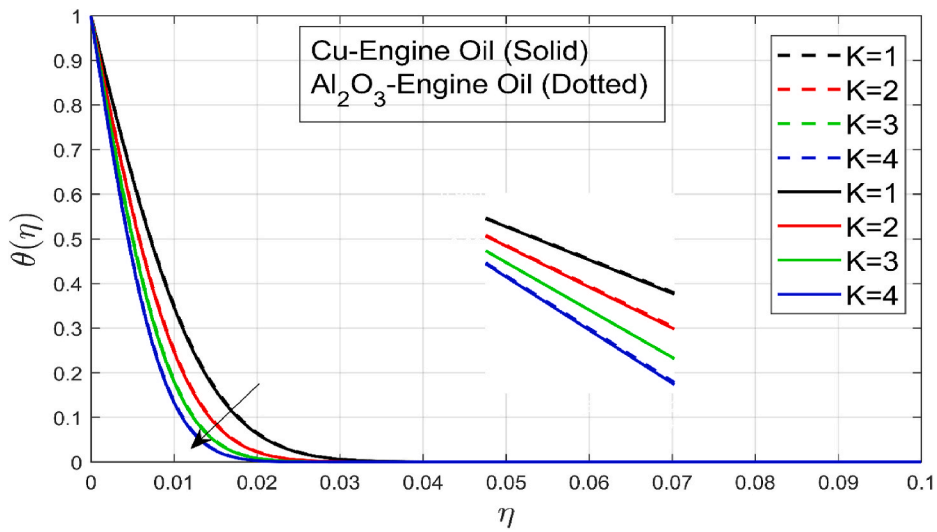


Fig. 5(a). The impact of slip K on temperature profile $\theta(\eta)$.

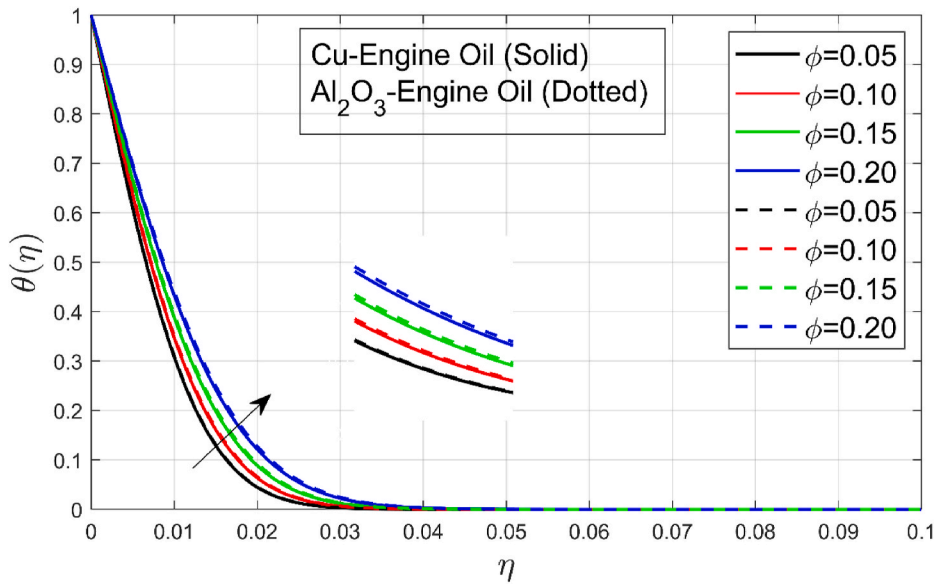


Fig. 5(b). The impact of volume fraction ϕ on temperature profile. $\theta(\eta)$.

Table 1
Thermo-Physical properties of Nanoparticles (Cu, Al_2O_3) and Base Fluid Engine oil.

Properties	Density (ρ)	Thermal Conductivity (K)	Specific Heat (C_p)
Cu	8933	400	385
Al_2O_3	3970	40	765
Engine oil	884	0.144	1910

Table 2
Variation of distinct parameters on skin friction and Nusselt number (ϕ, K) for $\lambda = 0.5, Pr = 6450$.

ϕ	K	Cu – Engine oil		Al_2O_3 – Engine oil	
		$-1/(1-\phi)^5/2f''(0)$	$-(kn/kf)\theta'(0)$	$-1/(1-\phi)^5/2f''(0)$	$-(kn/kf)\theta'(0)$
0.0	0.0	10.0375	67.9228	10.0375	61.7912
	0.2	12.0473	67.9228	12.0473	67.9228
	0.4	14.0601	73.5584	14.0601	73.5584
	0.6	16.0759	78.8019	16.0759	78.8019
0.1	0.0	13.0851	78.9472	13.0641	78.8015
	0.2	15.7065	86.8434	15.68	86.682
	0.4	18.3337	94.099	18.30	93.9234
0.2	0.0	20.9666	100.848	20.924	100.66
	0.2	17.575	101.973	17.5329	101.547
	0.4	21.0965	112.291	21.0435	111.817
0.4	24.6265	121.768	24.5591	121.252	
	0.6	28.1649	130.581	28.0798	130.026

Table 3

Variation of distinct parameters on skin friction and Nusselt number (φ, λ) for $K = 0.5, Pr = 6450$.

λ	φ	<i>Cu – Engine oil</i>		<i>Al₂O₃ – Engine oil</i>	
		$-1/(1-\varphi)^{5/2} f''(0)$	$-(kn/kf) \theta'(0)$	$-1/(1-\varphi)^{5/2} f''(0)$	$-(kn/kf) \theta'(0)$
0.0	0.0	36.7941	304.275	36.7941	298.858
	0.1	36.8901	259.665	36.8016	255.592
	0.2	36.9201	216.203	36.7884	213.402
	0.3	36.9027	170.033	36.7611	168.637
0.1	0.0	36.786	304.273	36.786	298.856
	0.1	36.8782	259.662	36.7932	255.59
	0.2	36.9071	216.2	36.7805	213.4
	0.3	36.9803	170.03	36.7543	168.635
0.2	0.0	36.7779	304.271	36.7779	298.855
	0.1	36.8663	259.659	36.7848	255.588
0.2	36.894	216.197	36.7726	213.398	
0.3	36.9878	170.028	36.7475	168.634	

Table 4

Comparison of present values of $f''(0)$ and $h'(0)$ with already published literature for $\lambda = K = 0$.

λ	<i>C.Y. Wang [48]</i>		<i>Nazar et al. [47]</i>		<i>Takhar & Nath [4]</i>		<i>Zaimi et al. [20]</i>		<i>Current Results</i>	
	$f''(0)$	$h'(0)$	$f''(0)$	$h'(0)$	$f''(0)$	$h'(0)$	$f''(0)$	$h'(0)$	$f''(0)$	$h'(0)$
0.0	1.0000	0.0000	1.0000	0.0000	1.0000	0.0000	1.0000	0.0000	1.0014	0.000000
0.2	1.0000	0.0000	1.0000	0.0000	1.0000	0.0000	1.0331	0.2385	1.03318	0.23856
0.4	1.0000	0.0000	1.0000	0.0000	1.0000	0.0000	1.009	0.4310	1.01011	0.43193
0.5	1.1384	0.5128	1.1384	0.5128	1.1383	0.5127	1.1384	0.5128	1.13889	0.51832
0.6	1.1384	0.5128	1.1384	0.5128	1.1383	0.5127	1.1764	0.5874	1.17676	0.58742
0.8	1.1384	0.5128	1.1384	0.5128	1.1383	0.5127	1.2518	0.7204	1.25189	0.72058
1.0	1.3250	0.8371	1.3250	0.8371	1.3250	0.8370	1.3250	0.8371	1.32596	0.83725
1.5	1.3250	0.8371	1.3250	0.8371	1.3250	0.8371	1.3250	0.8371	1.49641	1.08299
2.0	1.6523	1.2873	1.6523	1.2873	1.6524	1.2870	1.6523	1.2873	1.65235	1.28726
2.5	1.6523	1.2873	1.6523	1.2870	1.6524	1.2870	1.6523	1.2873	1.79573	1.46522
3.0	1.6523	1.2873	1.6523	1.2870	1.6523	1.2870	1.9289	1.6248	1.92893	1.62474

Table 5

Comparison of present values of $\theta'(0)$ with already published literature for $\lambda = K = 0$.

<i>Pr</i>	$\lambda = 0.0$			$\lambda = 0.5$			$\lambda = 2.0$		
	Present Results	Wang [47]	Kumari [21]	Present Results	Wang [47]	Kumara [21]	Present Results	Wang [47]	Kumari [21]
0.7	0.47159	0.455	0.4560	0.42905	0.390	0.3903	0.33829	0.242	0.2549
2.0	0.91168	0.911	0.9117	0.85325	0.853	0.8530	0.65527	0.638	0.6382
7.0	1.89553	1.894	1.8977	1.85120	1.850	1.8561	1.66437	1.664	1.6684

5. Graphs of skin friction and Nusselt Number

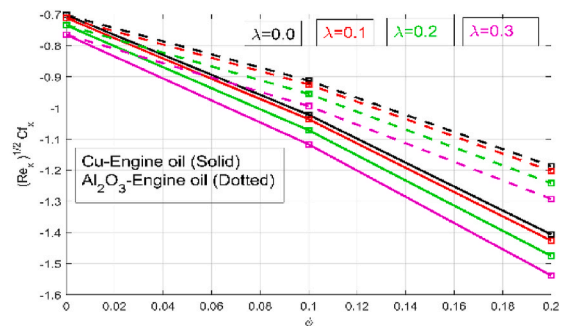
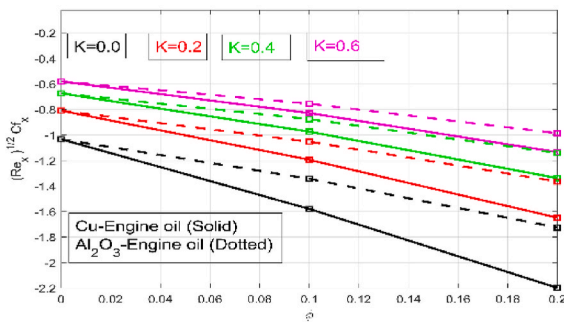


Fig. 6(a). Skin friction C_{fx} for different values of λ and K

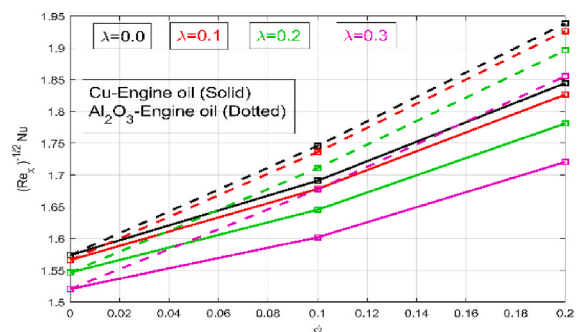
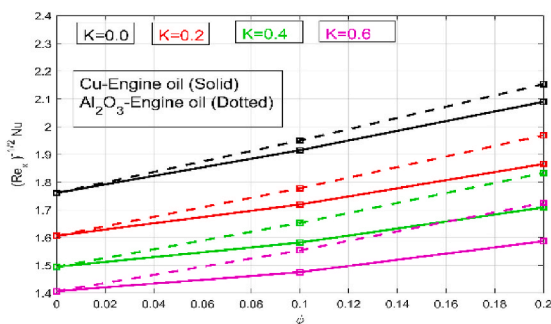


Figure 6(b). Nusselt Number Nu_x for different values of λ and K

6. Conclusions

In this analysis, the partial slip influence on 3D rotational engine oil-based nanofluid movement on linear extending is thoroughly analyzed. PDEs are transformed into ODEs by using transformation. Numerical results are obtained by using the bvp4c technique at MATLAB. Further deductions can be made as follows:

1. Rotation and partial slip decrease the velocity and increase the temperature of both nanofluids.
2. A rise in temperature profile because of particle volume concentration ϕ is found to be less prominent in Al_2O_3 – Engine oil and more in the case of Cu – Engine oil nanofluid.
3. An increase in velocity slip parameter K results in a rise in heat flux and skin friction for both nanofluids.
4. The volumetric concentration of nanoparticles ϕ decays the velocity of Cu – Engine oil more related to Al_2O_3 – Engine oil nanofluid.
5. A higher rate of angular velocity implies a higher heat transmission rate and lower skin friction.
6. Cu Nanoparticles proved to be better heat carriers than Al_2O_3 nanoparticles.
7. Our applied numerical scheme is up to the mark as compared to already published literature.

Authorship contributions

Azad Hussain: Conceptualization, Formal analysis; Mubashir Arshad: Investigation, Methodology; Ali Hassan: Resources; Aysha Rehman: Software, Writing - original draft; Validation, Hijaz Ahmad, Visualization, Writing - review and editing; Jamel Baili: Writing - review and editing, Project administration; Tuan Nguyen Gia: Funding acquisition, Visualization.

Funding

This research work was supported by the Deanship of Scientific Research at King Khalid University under Grant number RGP. 1/155/42.

Contributions of authors

All authors contributed equally.

Declaration of competing interest

The author confirms that this article has no conflict of interest.

Acknowledgments

The authors extend their thanks to the Deanship of Scientific Research at King Khalid University Saudi Arabia for funding this work through the big research groups under grant number RGP. 1/155/42.

References

- [1] L.J. Crane, Flow past a stretching plate, *Zeitschrift für angewandte Mathematik und Physik ZAMP* 21 (4) (1970) 645–647.
- [2] C.Y. Wang, Analysis of viscous flow due to a stretching sheet with surface slip and suction, *Nonlinear Anal. R. World Appl.* 10 (1) (2009) 375–380.
- [3] B.S. Dandapat, A.S. Gupta, Flow and heat transfer in a viscoelastic fluid over a stretching sheet, *Int. J. Non Lin. Mech.* 24 (3) (1989) 215–219.
- [4] H.S. Takhar, G. Nath, Unsteady flow over a stretching surface with a magnetic field in a rotating fluid, *Z. Angew. Math. Phys.* 49 (6) (1998) 989–1001.
- [5] K. Vajravelu, A. Hadjinicolaou, Heat transfer in a viscous fluid over a stretching sheet with viscous dissipation and internal heat generation, *Int. Commun. Heat Mass Tran.* 20 (3) (1993) 417–430.
- [6] G.H. Atefi, H. Niazmand, M.R. Meigounpoory, Numerical analysis of 3-D flow past a stationary sphere with slip condition at low and moderate Reynolds numbers, *J. Dispersion Sci. Technol.* 28 (4) (2007) 591–602.
- [7] A. Hussain, M.A. Elkothb, M. Arshad, A. Rehman, K. Soopy Nisar, A. Hassan, C.A. Saleel, Computational investigation of the combined impact of nonlinear radiation and magnetic field on three-dimensional rotational nanofluid flow across a stretchy surface, *Processes* 9 (8) (2021) 1453.
- [8] A. Hussain, M. Arshad, A. Rehman, A. Hassan, S.K. Elagan, N.A. Alshehri, Heat transmission of engine-oil-based rotating nanofluids flow with influence of partial slip condition: a computational model, *Energies* 14 (13) (2021) 3859.
- [9] A. Hussain, M. Arshad, A. Rehman, A. Hassan, S.K. Elagan, H. Ahmad, A. Ishan, Three-dimensional water-based magneto-hydrodynamic rotating nanofluid flow over a linear extending sheet and heat transport analysis: a numerical approach, *Energies* 14 (16) (2021) 5133.
- [10] S. Nadeem, A.U. Rehman, R. Mehmood, Boundary layer flow of rotating two phase nanofluid over a stretching surface, *Heat Tran. Asian Res.* 45 (3) (2016) 285–298.
- [11] Z.A. Nima, A. Biswas, I.S. Bayer, F.D. Hardcastle, D. Perry, A. Ghosh, A.S. Biris, Applications of surface-enhanced Raman scattering in advanced bio-medical technologies and diagnostics, *Drug Metab. Rev.* 46 (2) (2014) 155–175.
- [12] I. Waini, A. Ishak, I. Pop, Unsteady flow and heat transfer past a stretching/shrinking sheet in a hybrid nanofluid, *Int. J. Heat Mass Tran.* 136 (2019) 288–297.
- [13] S.U. Choi, J.A. Eastman, *Enhancing Thermal Conductivity of Fluids with Nanoparticles* (No. ANL/MSD/CP-84938; CONF-951135-29), Argonne National Lab., IL (United States), 1995.
- [14] S. Lee, S.S. Choi, S.A. Li, J.A. Eastman, *Measuring Thermal Conductivity of Fluids Containing Oxide Nanoparticles*, 1999.
- [15] B. Li, L. Zheng, X. Zhang, Heat transfer in pseudo-plastic non-Newtonian fluids with variable thermal conductivity, *Energy Convers. Manag.* 52 (1) (2011) 355–358.
- [16] B.C. Pak, Y.I. Cho, "Hydrodynamic and heat transfer study of dispersed fluids with submicron metallic oxide particles", *Experimental Heat Transfer an International Journal* 11 (2) (1998) 151–170.
- [17] M. Kumari, G. Nath, "Analytical solution of unsteady three-dimensional MHD boundary layer flow and heat transfer due to impulsively stretched plane surface", *Commun. Nonlinear Sci. Numer. Simulat.* 14 (8) (2009) 3339–3350.
- [18] A. Hussain, A. Hassan, Q. Al Mdallal, H. Ahmad, A. Rehman, M. Altanji, M. Arshad, Heat transport investigation of magneto-hydrodynamics (SWCNT-MWCNT) hybrid nanofluid under the thermal radiation regime, *Case Studies in Thermal Engineering* 27 (2021) 101244.
- [19] A. Shafiq, G. Rasool, C.M. Khaliq, "Significance of thermal slip and convective boundary conditions in three dimensional rotating Darcy-Forchheimer nanofluid flow", *Symmetry* 12 (no5) (2020) 741.
- [20] K. Zaimi, A. Ishak, I. Pop, Stretching surface in rotating viscoelastic fluid, *Appl. Math. Mech.* 34 (8) (2013) 945–952.
- [21] M. Kumari, G. Nath, Transient rotating flow over a moving surface with a magnetic field, *Int. J. Heat Mass Tran.* 48 (14) (2005) 2878–2885.
- [22] H.S. Takhar, A.J. Chamkha, G. Nath, Flow and mass transfer on a stretching sheet with a magnetic field and chemically reactive species, *Int. J. Eng. Sci.* 38 (12) (2000) 1303–1314.
- [23] F. Mebarek-Oudina, Convective heat transfer of Titania nanofluids of different base fluids in cylindrical annulus with discrete heat source, *Heat Tran. Asian Res.* 48 (1) (2019) 135–147.
- [24] W. Abbas, M.M. Magdy, Heat and mass transfer analysis of nanofluid flow based on, and over a moving rotating plate and impact of various nanoparticle shapes, *Math. Probl Eng.* (2020).
- [25] A. Hussain, M.H. Alshbool, A. Abdussattar, A. Rehman, H. Ahmad, T.A. Nofal, M.R. Khan, A computational model for hybrid nanofluid flow on a rotating surface in the existence of convective condition, *Case Studies in Thermal Engineering* (2021) 101089.
- [26] K. Swain, F. Mebarek-Oudina, S.M. Abo-Dahab, Influence of MWCNT/Fe 3 O 4 hybrid nanoparticles on an exponentially porous shrinking sheet with chemical reaction and slip boundary conditions, *J. Therm. Anal. Calorim.* (2021) 1–10.
- [27] A. Hussain, A. Rehman, S. Nadeem, M.R. Khan, A. Issakhov, A Computational Model for the Radiated Kinetic Molecular Postulate of Fluid-Originated Nanomaterial Liquid Flow in the Induced Magnetic Flux Regime, *Mathematical Problems in Engineering*, 2021, 2021.
- [28] C.J. Zhou, A. Abidi, Q.H. Shi, M.R. Khan, A. Rehman, A. Issakhov, A.M. Galal, Unsteady radiative slip flow of MHD Casson fluid over a permeable stretched surface subject to a non-uniform heat source, *Case Studies in Thermal Engineering* (2021) 101141.
- [29] A. Hussain, M.H. Alshbool, A. Abdussattar, A. Rehman, H. Ahmad, T.A. Nofal, M.R. Khan, A computational model for hybrid nanofluid flow on a rotating surface in the existence of convective condition, *Case Studies in Thermal Engineering* (2021) 101089.
- [30] A. Rehman, A. Hussain, S. Nadeem, Assisting and opposing stagnation point pseudoplastic nano liquid flow towards a flexible Riga sheet: a computational approach, *Math. Probl Eng.* (2021), 2021.

- [31] N. Abbas, S. Saleem, S. Nadeem, A.A. Alderremy, A.U. Khan, On stagnation point flow of a micro polar nanofluid past a circular cylinder with velocity and thermal slip, *Results in Physics* 9 (2018) 1224–1232.
- [32] A. Hussain, A. Rehman, S. Nadeem, M.Y. Malik, A. Issakhov, L. Sarwar, S. Hussain, A combined convection carreau–yasuda nanofluid model over a convective heated surface near a stagnation point: a numerical study, *Math. Probl Eng.* (2021), 2021.
- [33] N. Abbas, M. Asim, N. Tariq, T. Baker, S. Abbas, A mechanism for securing IoT-enabled applications at the fog layer, *J. Sens. Actuator Netw.* 8 (1) (2019) 16.
- [34] A. Rehman, A. Hussain, S. Nadeem, Physical aspects of convective and radiative molecular theory of liquid originated nanofluid flow in the existence of variable properties, *Phys. Scripta* 96 (3) (2021), 035219.
- [35] S. Nadeem, N. Abbas, M.Y. Malik, Inspection of hybrid based nanofluid flow over a curved surface, *Comput. Methods Progr. Biomed.* 189 (2020) 105193.
- [36] N. Abbas, S. Nadeem, A. Saleem, M.Y. Malik, A. Issakhov, F.M. Alharbi, Models base study of inclined MHD of hybrid nanofluid flow over nonlinear stretching cylinder, *Chin. J. Phys.* 69 (2021) 109–117.
- [37] A. Hussain, Q. Haider, A. Rehman, H. Ahmad, J. Baili, N.H. Aljahdaly, A. Hassan, A thermal conductivity model for hybrid heat and mass transfer investigation of single and multi-wall carbon nano-tubes flow induced by a spinning body, *Case Studies in Thermal Engineering* (2021) 101449.
- [38] M.N. Khan, S. Nadeem, N. Abbas, A.M. Zidan, Heat and mass transfer investigation of a chemically reactive Burgers nanofluid with an induced magnetic field over an exponentially stretching surface, *Proc. IME E J. Process Mech. Eng.* (2021), 09544089211034941.
- [39] A. Baslem, G. Sowmya, B.J. Gireesha, B.C. Prasannakumara, M. Rahimi-Gorji, N.M. Hoang, Analysis of thermal behavior of a porous fin fully wetted with nanofluids: convection and radiation, *J. Mol. Liq.* 307 (2020) 112920.
- [40] M.W. Alam, S. Bhattacharyya, B. Souayah, K. Dey, F. Hammami, M. Rahimi-Gorji, R. Biswas, CPU heat sink cooling by triangular shape micro-pin-fin: numerical study, *Int. Commun. Heat Mass Tran.* 112 (2020) 104455.
- [41] R.P. Gowda, R.N. Kumar, A. Aldalbahi, A. Issakhov, B.C. Prasannakumara, M. Rahimi-Gorji, M. Rahaman, Thermophoretic particle deposition in time-dependent flow of hybrid nanofluid over rotating and vertically upward/downward moving disk, *Surfaces and Interfaces* 22 (2021) 100864.
- [42] K.G. Kumar, A. Baslem, B.C. Prasannakumara, J. Majdoubi, M. Rahimi-Gorji, S. Nadeem, Significance of Arrhenius activation energy in flow and heat transfer of tangent hyperbolic fluid with zero mass flux condition, *Microsyst. Technol.* 26 (8) (2020) 2517–2526.
- [43] S.C. Saha, M.S. Islam, M. Rahimi-Gorji, M.M. Molla, Aerosol particle transport and deposition in a CT-scan based mouth-throat model, No. 1, in: *AIP Conference Proceedings*, vol. 2121, 2019, July, p. 40011 (AIP Publishing LLC).
- [44] A. Zeeshan, Z. Ali, M.R. Gorji, F. Hussain, S. Nadeem, Flow analysis of biconvective heat and mass transfer of two-dimensional couple stress fluid over a paraboloid of revolution, *Int. J. Mod. Phys. B* 34 (11) (2020) 2050110.
- [45] A. Bit, A. Ablawi, H. Chattopadhyay, Q.A. Quais, A.C. Benim, M. Rahimi-Gorji, H.T. Do, Three dimensional numerical analysis of hemodynamic of stenosed artery considering realistic outlet boundary conditions, *Comput. Methods Progr. Biomed.* 185 (2020) 105163.
- [46] S. Nadeem, A. Ur Rehman, R. Mehmood, M. Adil Sadiq, Partial Slip effects on a rotating flow of two phase nano fluid over a stretching surface, *Curr. Nanosci.* 10 (6) (2014) 846–854.
- [47] C.Y. Wang, Stretching a surface in a rotating fluid, *Zeitschrift für angewandte Mathematik und Physik ZAMP* 39 (2) (1988) 177–185.